

MOL 18960

Lysophosphatidylserine stimulates L2071 mouse fibroblast chemotactic migration via a process involving pertussis toxin-sensitive trimeric G proteins

Kyoung Sun Park, Ha-Young Lee, Mi-Kyoung Kim, Eun Ha Shin, Seong Ho Jo, Sang Doo Kim, Dong-Soon Im, and Yoe-Sik Bae

Medical Research Center for Cancer Molecular Therapy and Department of Biochemistry, College of Medicine, Dong-A University, Busan, 602-714, Korea (K.S.P., H.-Y.L., M.-K.K., E.H.S., S.H.J., S.D.K., Y.-S.B.); College of Pharmacy, Pusan National University, Busan, 609-735, Korea (D.-S.I.).

MOL 18960

Running Title: Lysophosphatidylserine-induced cell migration

Corresponding author: Yoe-Sik Bae, Medical Research Center for Cancer Molecular Therapy  
and Department of Biochemistry, College of Medicine, Dong-A University, Busan 602-714,  
Korea. Tel: 82-51-240-2889; Fax: 82-51-241-6940; e-mail: yoesik@donga.ac.kr

The number of text pages: 29      The number of figures: 9  
The number of references: 43      The number of words in the Abstract: 239  
The number of words in the Introduction: 413  
The number of words in the Discussion: 949

Abbreviations used in this paper: S1P, sphingosine 1-phosphate; LPC, lysophosphatidylcholine; SPC, sphingosylphosphorylcholine; GPCR, G-protein-coupled receptor; LPS, lysophosphatidylserine; fura-2/AM, fura-2 pentaacetoxymethylester; BAPTA/AM, 1,2-*bis*(*o*-Aminophenoxy)ethane-N,N,N',N'-tetraacetic Acid Tetra(acetoxymethyl) Ester; U-73122, 1-[6-((17 $\beta$ -3-Methoxyestra-1,3,5(10)-trien-17-yl)amino)hexyl]-1H-pyrrole-2,5-dione; U-73343, 1-[6-((17 $\beta$ -3-Methoxyestra-1,3,5(10)-trien-17-yl)amino)hexyl]-2,5-pyrrolidinedione; LY294002, 2-(4-Morpholinyl)-8-phenyl-4H-1-benzopyran-4-one; PD98059, 2'-Amino-3'-methoxyflavone; SB203580, 4-(4-Fluorophenyl)-2-(4-methylsulfonylphenyl)-5-(4-pyridyl)-1H-imidazole; RGS, regulators of G-protein signaling; MAPK, mitogen-activated protein kinase; ERK, extracellular signal regulated protein kinase; PI3K, phosphoinositide 3-kinase.

## Abstract

Lysophosphatidylserine (LPS) may be generated after phosphatidylserine-specific phospholipase A<sub>2</sub> activation. However, the effects of LPS on cellular activities and the identities of its target molecules have not been fully elucidated. In this study, we observed that LPS stimulates an intracellular calcium increase in L2071 mouse fibroblast cells, and that this increase was inhibited by 1-[6-((17 $\beta$ -3-Methoxyestra-1,3,5(10)-trien-17-yl)amino)hexyl]-1H-pyrrole-2,5-dione (U-73122) but not by pertussis toxin, suggesting that LPS stimulates calcium signaling via G-protein coupled receptor-mediated phospholipase C activation. Moreover, LPS-induced calcium mobilization was not inhibited by the lysophosphatidic acid receptor antagonist, (S)-Phosphoric acid mono-{2-octadec-9-enoylamino-3-[4-(pyridine-2-ylmethoxy)-phenyl]-propyl} ester (VPC 32183), thus indicating that LPS binds to a receptor other than lysophosphatidic acid receptors. It was also found that LPS stimulates two types of mitogen-activated protein kinase, namely, extracellular signal-regulated protein kinase (ERK) and p38 kinase, in L2071 cells. Furthermore, these LPS-induced ERK and p38 kinase activations were inhibited by pertussis toxin, which suggests the role of pertussis toxin-sensitive G-proteins in the process. In terms of functional issues, LPS stimulated L2071 cell chemotactic migration, which was completely inhibited by pertussis toxin, indicating the involvement of pertussis toxin-sensitive G<sub>i</sub> protein(s). This chemotaxis of L2071 cells induced by LPS was also dramatically inhibited by 2-(4-Morpholinyl)-8-phenyl-4H-1-benzopyran-4-one (LY294002) and by 2'-Amino-3'-methoxyflavone (PD98059). This study demonstrates that LPS stimulates at least two different signaling cascades, one of which involves a pertussis toxin-insensitive but phospholipase C-dependent intracellular calcium increase, and the other, a pertussis toxin-sensitive chemotactic migration mediated by phosphoinositide 3-kinase and ERK.

## Introduction

Lyso-type phospholipid molecules, such as, lysophosphatidic acid, sphingosine 1-phosphate (S1P), lysophosphatidylcholine (LPC), and sphingosylphosphorylcholine (SPC) have attracted the attentions of researchers for over two decades. In particular, the identification of lysophosphatidic acid as a cell proliferating factor in serum proved to be a landmark event, and the involvement of S1P in angiogenesis has been intensively studied (van Corven et al., 1989; Tigyi et al., 1994; Lee et al., 1999). Moreover, the discovery of the EDG family of G-protein-coupled receptors (GPCR) of lysophosphatidic acid and S1P triggered a variety of pathophysiological studies on lysophospholipids in many cell and tissue types (Hla and Maciag, 1990; Lee et al., 1998; Fukushima et al., 1998). Moreover, the OGR1 GPCR family has been reported to contain SPC, LPC, and psychosine receptors, although the GPCRs were recently re-evaluated and found to be composed largely of proton-sensing GPCRs (Xu et al., 2000; Zhu et al., 2001). In addition, GPR23, GPR12, and GPR119 have been suggested to be lysophosphatidic acid, SPC, and LPC receptors, respectively (Noguchi et al., 2003; Ignatov et al., 2003; Soga et al., 2005). However, in contrast to the many studies that have demonstrated the pivotal roles of the above-mentioned lysophospholipids in biological responses, the roles of other lysophospholipids, like lysophosphatidylserine (LPS), have not been elucidated.

Lysophosphatidylserine (LPS) is generated by activated platelets (Sato et al., 1997). Moreover, previous studies have demonstrated that platelets contain serine-phospholipid-selective phospholipase, which is secreted by activated platelets and specifically acts on phosphatidylserine to induce LPS production (Sato et al., 1997). High concentrations of LPS have also been found in the ascites of ovarian cancer patients and in lacrimal fluid after corneal injury (Xu et al., 1995a; Liliom et al., 1998). LPS has also been reported to induce a

## MOL 18960

transient increases in intracellular calcium in ovarian and breast cancer cell lines (Xu et al., 1995a), to stimulate IL-2 production in Jurkat T cells, and to inhibit Jurkat cell proliferation (Xu et al., 1995b). Furthermore, LPS treatment enhanced NGF-induced histamine release in rat mast cells and the NGF-induced differentiation of PC12 cells (Kawamoto et al., 2002; Luorensen and Blennerhassett, 1998). Although the target molecules of LPS have not been identified, its actions are believed not to be mediated via the known GPCRs of lysophosphatidic acid, S1P, or LPC.

In this study, we investigated LPS-induced cell migration and its signaling pathways in L2071 mouse fibroblasts, and found that this effect is mediated by two separate signaling pathways with the involvement of pertussis toxin-sensitive trimeric G proteins.

## Materials and methods

### Cell line and reagents

L2071 mouse fibroblasts were cultured in RPMI 1640 medium with 10% FBS, 1% sodium bicarbonate buffer, and 1% HEPES buffer. 1-acyl-2-hydroxy-*sn*-glycero-3-phospho-L-serine, 1-acyl-2-hydroxy-*sn*-glycero-3-phosphoethanolamine, S1P, lysophosphatidic acid, leukotriene B<sub>4</sub>, and (S)-Phosphoric acid mono-{2-octadec-9-enoylamino-3-[4-(pyridine-2-ylmethoxy)-phenyl]-propyl} ester (Ammonium Salt) (VPC 32183) were purchased from Avanti Polar Lipids, Inc. (Alabaster, Alabama). Fura-2 pentaacetoxymethylester (fura-2/AM) and 1,2-*bis*(*o*-Aminophenoxy)ethane-N,N,N',N'-tetraacetic Acid Tetra(acetoxymethyl) Ester (BAPTA/AM) were purchased from Molecular Probes (Eugene, OR). 1-[6-((17 $\beta$ -3-Methoxyestra-1,3,5(10)-trien-17-yl)amino)hexyl]-1H-pyrrole-2,5-dione (U-73122), 1-[6-((17 $\beta$ -3-Methoxyestra-1,3,5(10)-trien-17-yl)amino)hexyl]-2,5-pyrrolidinedione (U-73343), and 2-(4-Morpholinyl)-8-phenyl-4H-1-benzopyran-4-one (LY294002) were purchased from

## MOL 18960

Calbiochem (San Diego, CA). Enhanced chemiluminescence reagents from Amersham Biosciences (Piscataway, NJ), Phospho-ERK1/2, phospho-p38 and ERK2 antibodies were purchased from New England Biolabs (Beverly, MA). Phospho-Akt antibody, Akt antibody, fibrinogen, and fibronectin were purchased from Sigma (St. Louis, MO). 2'-Amino-3'-methoxyflavone (PD98059) and 4-(4-Fluorophenyl)-2-(4-methylsulfonylphenyl)-5-(4-pyridyl)-1H-imidazole (SB203580) were obtained from Biomol (Plymouth Meeting, PA) and were dissolved in dimethyl sulfoxide before being added to the cell culture. The final concentrations of dimethyl sulfoxide in culture were 0.1% or less.

### **Ca<sup>2+</sup> measurement**

Intracellular calcium concentration was determined by Grynkiewicz's method using fura-2/AM (Grynkiewicz et al., 1985; Bae et al., 2001). Briefly, prepared cells were incubated with 3  $\mu$ M fura-2/AM at 37°C for 50 min in fresh serum free RPMI 1640 medium with continuous stirring.  $2 \times 10^6$  cells were aliquoted for each assay into Locke's solution (154 mM NaCl, 5.6 mM KCl, 1.2 mM MgCl<sub>2</sub>, 5 mM HEPES, pH 7.3, 10 mM glucose, 2.2 mM CaCl<sub>2</sub>, and 0.2 mM EGTA). Fluorescence was measured at 500 nm at excitation wavelengths of 340 nm and 380 nm.

### **Stimulation of cells with LPS for Western blot analysis**

Cultured cells ( $2 \times 10^6$ ) were stimulated with the indicated concentrations of LPS for the predetermined lengths of time. After stimulation, the cells were washed with serum free RPMI 1640 medium and lysed in lysis buffer (20 mM Hepes, pH 7.2, 10% glycerol, 150 mM NaCl, 1% Triton X-100, 50 mM NaF, 1 mM Na<sub>3</sub>VO<sub>4</sub>, 10  $\mu$ g/ml leupeptin, 10  $\mu$ g/ml aprotinin, and 1 mM phenylmethylsulfonyl fluoride). Detergent insoluble materials were pelleted by centrifugation (12,000 x g, 15 min, at 4°C), and the soluble supernatant fraction

MOL 18960

was removed and stored at either -80°C or used immediately. Protein concentrations in the lysates were determined using Bradford protein assay reagent.

### **Electrophoresis and immunoblot analysis**

Protein samples were prepared for electrophoresis then separated using a 10% SDS-polyacrylamide gel and the buffer system described previously (Kim et al., 2003). Following the electrophoresis, the proteins were blotted onto nitrocellulose membrane, which was blocked by incubating with TBST (Tris-buffered saline, 0.05% Tween-20) containing 5% non-fat dried milk. The membranes were then incubated with anti-phospho-ERK antibody, anti-phospho-p38 kinase antibody or anti-ERK antibody and washed with TBST. Antigen-antibody complexes were visualized after incubating the membrane with 1:5000 diluted goat anti-rabbit IgG or goat anti-mouse IgG antibody coupled to horseradish peroxidase using the enhanced chemiluminescence detection system.

### **Transient transfection of regulators of G-protein signaling (RGS)4**

HA tagged human wild type RGS4 cDNA was obtained from UMR cDNA Resource Center (Rolla, Mo). Transfections were performed using LipofectAMINE reagents (Invitrogen Corporation) according to the manufacturer's instructions. The cells were harvested 48 h after transfection and expression of HA-tagged RGS4 protein was examined by Western blotting using monoclonal anti-HA antibody (Sigma) (data not shown).

### **Chemotaxis assay**

Chemotaxis assays were performed using multiwell chambers (Neuroprobe Inc., Gaithersburg, MD) as described previously (Bae et al., 2003). Briefly, polycarbonate filters (8 µm pore size) were precoated with 20 µg/ml of BSA, 20 µg/ml of fibrinogen, or 20 µg/ml of

## MOL 18960

fibronectin in HEPES-buffered RPMI 1640 medium. A dry coated filter was placed on a 96-well chamber containing different concentrations of peptides. L2071 cells were suspended in RPMI at a concentration of  $1 \times 10^6$  cells / ml, and 25  $\mu$ l of the cell suspension were placed onto the upper well of the chamber. After incubation for 4 h at 37°C, non-migrating cells were removed by scarping, and cells that migrated across the filter were dehydrated, fixed, and stained with hematoxylin (Sigma, St. Louis, MO). The stained cells in three randomly chosen high power fields (HPF, 400 x) were then counted for each well.

### Statistics

The results are expressed as means  $\pm$  SE of the number of determinations indicated. Statistical significance of differences was determined by ANOVA. Significance was accepted when  $P < 0.05$ .

### Results

#### LPS stimulates calcium mobilization in L2071 mouse fibroblast cells

The activations of some lysolipids GPCRs, such as S1P<sub>2</sub> or LPA<sub>3</sub>, are associated with phospholipase C activation, subsequent inositol-1,4,5-trisphosphate production, and intracellular calcium elevation (Kon et al., 1999; An et al., 1998). To examine whether L2071 cells express GPCR(s) for LPS, we examined the effects of LPS on intracellular calcium in L2071 cells. As shown in Figure 1A, the stimulation of L2071 with 2  $\mu$ M LPS caused an intracellular calcium elevation in the presence or absence of extracellular calcium. However, lysophosphatidylethanolamine, which has a chemical structure resembling that of LPS, did not affect intracellular calcium concentrations in these cells (Fig. 1A). We also investigated the concentration-dependency of this LPS-induced intracellular calcium increase, and



observed this effect after treating L2071 cells with 10 nM of LPS; maximal activity was observed at 0.5 -1  $\mu$ M (Fig. 1B).

### **LPS-stimulated calcium mobilization is U-73122-sensitive but pertussis toxin-insensitive**

Phospholipase C-dependent inositol-1,4,5-trisphosphate-mediated response is a well-known mechanism of intracellular calcium increase in the absence of extracellular calcium (Noh et al., 1995). To determine the role of phospholipase C on LPS-induced intracellular calcium elevation, we pretreated L2071 cells with the specific phospholipase C inhibitor U-73122, or with its inactive analogue U-73343. Figure 2A demonstrates that U-73122, but not U-73343, completely inhibited LPS-induced intracellular calcium increase, indicating that LPS stimulates intracellular calcium elevation via phospholipase C activation in L2071 cells.

We also investigated the role of pertussis toxin-sensitive G-proteins on LPS-induced intracellular calcium elevation. Cultured L2071 cells were preincubated with 100 ng/ml of pertussis toxin prior to being stimulated with 2  $\mu$ M LPS. However, this pertussis toxin pretreatment did not block intracellular calcium elevation by LPS (Fig. 2B), demonstrating that LPS induces intracellular calcium elevation in a pertussis toxin-insensitive manner.

To confirm whether pertussis toxin sufficiently inhibits G $\alpha$ i-mediated signaling, we examined the effect of pertussis toxin on leukotriene B<sub>4</sub>-induced intracellular calcium elevation in L2071 cells. As shown in Fig. 2B, leukotriene B<sub>4</sub> also stimulated calcium increase in L2071 cells, and this increase was completely inhibited by pertussis toxin, indicating that leukotriene B<sub>4</sub> induces intracellular calcium elevation in a pertussis toxin-sensitive manner in these cells (Fig. 2B). We also examined the effect of pertussis toxin at various concentrations on LPS-induced cytosolic calcium increases, and observed that the presence of pertussis toxin had no effect on LPS-induced cytosolic calcium increases (Fig.

2C), which suggests that LPS induces pertussis toxin-insensitive phospholipase C activation and cytosolic calcium increase.

### **LPS-induced intracellular calcium elevation is inhibited by lysophosphatidic acid or S1P**

Lysophosphatidic acid and S1P are known to upregulate intracellular calcium in a pertussis toxin-insensitive manner in mouse fibroblasts (van Corven et al., 1989; Im et al., 1997). Thus, we suspected that LPS utilizes the GPCRs of lysophosphatidic acid or S1P to elicit this  $\text{Ca}^{2+}$  response. As shown in Figure 3A, the stimulation of L2071 cells with LPS desensitized cells to a second LPS stimulation, indicating homologous desensitization. This was also observed for lysophosphatidic acid and for S1P. However, LPS-desensitized L2071 cells responded to lysophosphatidic acid and to S1P (Fig. 3A). Conversely, lysophosphatidic acid- or S1P-desensitized L2071 cells did not respond to LPS, indicating heterologous desensitization. These results suggest that LPS shares lysophosphatidic acid or S1P receptors or that the downstream signaling pathways converge or interact with those of lysophosphatidic acid or S1P.

We examined the possibility that LPS acts on lysophosphatidic acid or S1P receptors in L2071 cells. Pretreatment with a maximal concentration of LPS (2  $\mu\text{M}$ ) did not significantly affect lysophosphatidic acid- or S1P-induced calcium release in L2071 cells (Fig. 3C and 3D). The above results suggest that LPS does not bind to lysophosphatidic acid or S1P receptors.

### **LPS interacts with a unique receptor not shared with lysophosphatidic acid**

In order to determine whether LPS has its own unique cell surface receptor, we utilized the

## MOL 18960

lysophosphatidic acid receptor-selective antagonist, VPC 32183. As shown in Fig. 4A, lysophosphatidic acid-induced intracellular calcium increase was completely inhibited by preincubating L2071 cells with 1  $\mu$ M of VPC 32183. However, LPS-induced calcium signaling was unaffected by VPC 32183 (1  $\mu$ M) (Fig. 4B). LPS-induced calcium rises by several concentrations were not significantly inhibited by 1  $\mu$ M of VPC 32183 (Fig. 4C). These results strongly indicate that LPS acts at a unique cell surface receptor.

### **LPS stimulates ERK and p38 kinase in L2071 cells**

Mitogen-activated protein kinase (MAPK) has been reported to mediate extracellular signals that target the nucleus in several cell types (Johnson and Lapadat, 2002). In this study, we used Western blot analysis with anti-phospho-specific antibodies against each enzyme to examine whether LPS stimulates MAPKs. When L2071 cells were stimulated with 2  $\mu$ M of LPS for different times, ERK phosphorylation levels were transiently increased, and showed maximal activity 2-5 min after stimulation (Fig. 5A) and returned to baseline 10 min after stimulation (Fig. 5A). Another important MAPK, p38 kinase, was also transiently activated by LPS stimulation in a time course resembling that of ERK activation (Fig. 5A). In addition, we also examined the concentration-dependencies of LPS-induced ERK and p38 kinase activations. When L2071 cells were stimulated with various concentrations of LPS, ERK and p38 kinase were found to be activated in a concentration-dependent manner (Fig. 5B). In the case of ERK activation, LPS caused significant activation at 500 nM and maximal activation at 1-2  $\mu$ M (Fig. 5B). p38 kinase was also activated by 500 nM LPS and this peaked at 1-2  $\mu$ M LPS (Fig. 5B).

### **MAPK activation by LPS is mediated by pertussis toxin-sensitive G-protein**

Here, we examined the effect of pertussis toxin, a specific inhibitor of Gi type G proteins, on LPS-induced MAPK phosphorylation. When L2071 cells were preincubated with 100 ng/ml of pertussis toxin, prior to being stimulated with 2  $\mu$ M LPS, LPS-induced ERK and p38 kinase phosphorylations were found to be almost completely inhibited (Fig. 6A), thus indicating that LPS stimulates MAPK activation via a pertussis toxin-sensitive pathway. To further support the role of Gi on LPS-induced signaling in L2071 cells, we examined the effect of the overexpression of RGS4 overexpression (RGS4 is a negative regulator of Gi) on LPS-stimulated ERK phosphorylation. As shown in Fig. 6B, RGS4 overexpression dramatically inhibited LPS-induced ERK phosphorylation. Since RGS4 inhibits signaling via Gi and Gq/11 (Berman et al., 1996; Huang et al., 1997), and because LPS-induced ERK phosphorylation was almost completely inhibited by pertussis toxin (Fig. 6A), our results indicate that LPS stimulates ERK phosphorylation via Gi.

### **LPS stimulates Akt activity in a pertussis toxin-sensitive manner**

Akt has been reported to play important roles in the regulation of several cellular responses, such as, cell migration and cell survival (Morales-Ruiz et al., 2001). Here, we used Western blot analysis with anti-phospho-specific antibodies against Akt to determine whether LPS stimulates Akt. When L2071 cells were stimulated with 2  $\mu$ M LPS for different times, Akt phosphorylation was transiently increased, showing maximal activity after 2-5 min of stimulation (Fig. 7A) and return to baseline 10 min after stimulation (Fig. 7A). In addition, we also examined the concentration-dependency of LPS-induced Akt activation. When L2071 cells were stimulated with different concentrations of LPS, Akt was activated in a concentration-dependent manner (Fig. 7B). At 100 nM LPS caused significant Akt activation and maximal activation was observed at 2  $\mu$ M (Fig. 7B).

We also examined the effect of pertussis toxin on LPS-induced Akt phosphorylation. When L2071 cells were preincubated with 100 ng/ml of pertussis toxin prior to being stimulated with 2  $\mu$ M LPS, LPS-induced Akt phosphorylation was found to be almost completely inhibited (Fig. 7C). The preincubation of L2071 cells with 100 ng/ml of pertussis toxin prior to stimulation with several concentrations of LPS for 2 min also completely inhibited Akt phosphorylation (Fig. 7D). These results indicate that LPS stimulates Akt activation via a pertussis toxin-sensitive pathway.

### **LPS induces mouse fibroblast chemotaxis**

Since intracellular signaling through several chemoattractant receptors is required for the activation of several integrins involved in leukocyte adhesion and migration (Wang et al., 2002), we investigated the effect of LPS on fibroblast migration on several specific extracellular matrices. It was found that LPS induced the chemotactic migration of mouse fibroblasts on fibronectin but not on fibrinogen or BSA (Fig. 8A). Fig 7B shows the concentration-responsive curve of LPS-induced mouse fibroblast migration, and shows maximal activity at 2-5  $\mu$ M (Fig. 8B). To distinguish between LPS-induced chemotaxis and chemokinesis, we performed migration assays in the absence or presence of LPS in the upper wells of Boyden chambers as described previously (Bae et al., 1999). As shown in Table 1, the addition of LPS (5  $\mu$ M) to the upper chamber reduced the LPS-induced migrations of L2071 cells to the lower well, thus demonstrating that LPS induces mouse fibroblast chemotaxis.

### **LPS induces mouse fibroblasts chemotaxis via pertussis toxin-sensitive G-proteins, ERK, and phosphoinositide 3-kinase (PI3K)-dependent signaling**

## MOL 18960

Since LPS-induced MAPK and Akt phosphorylations were inhibited by pertussis toxin in L2071 cells, we examined the effect of pertussis toxin on LPS-induced mouse fibroblast chemotaxis. When L2071 cells were preincubated with 100 ng/ml of pertussis toxin prior to chemotaxis assays, the numbers of cell migrating toward LPS was reduced by > 95% (Fig. 9A), which strongly suggested the involvement of pertussis toxin-sensitive G proteins.

Several reports have shown that several chemoattractants stimulate PI3K-mediated Akt activity and that the PI3K pathway is involved in the chemotaxis of leukocytes stimulated by these chemoattractants (Haribabu et al., 1999; Lachance et al., 2002). Since we observed that LPS treatment caused a rapid increase in Akt phosphorylation in L2071 cells (Fig. 7), we investigated whether the PI3K pathway is required for LPS-induced L2071 chemotaxis. The preincubation of cells with LY294002 (50  $\mu$ M), a well-known PI3K inhibitor, for 15 min at 37°C prior to stimulation with LPS, was found to affect cellular chemotaxis (Fig. 9B), indicating that LPS activates the PI3K pathway and that this signaling is required for the LPS-induced chemotaxis of L2071 mouse fibroblast cells.

We also examined the roles of ERK and p38 kinase on LPS-induced L2071 chemotaxis. When L2071 cells were preincubated with PD98059 (50  $\mu$ M) or SB203580 (20  $\mu$ M) prior to chemotaxis assays, LPS-induced L2071 chemotaxis was found to be significantly blunted by PD98059, but not by SB203580 (Fig. 9B), implying that ERK-mediated signaling is involved in LPS-induced L2071 chemotaxis.

## Discussion

Fibroblast migration is associated with damaged tissue remodeling. In response to tissue damage or inflammation, fibroblasts migrate into inflammatory sites along cross-linked fibrin and fibronectin in the extracellular matrix (Hotary et al., 2002; Wilberding et al., 2001).

# MOL 18960

Fibroblast migration is important for the remodeling of the provisional extracellular matrix, as fibroblasts provide a fibrous attachment for growing tissue, and wound healing (Hotary et al., 2002; Wilberding et al., 2001), and thus the modulation of chemotactic migration is an important aspect of the cell biology of fibroblasts. Several groups have reported that various extracellular stimuli are involved in the regulation of fibroblast chemotactic migration (Kundra et al., 1994; Hama et al., 2004). However, the role of LPS in chemotaxis has not been studied. In the present study, we found for the first time that LPS, a lysophospholipid, stimulates the chemotactic migration of mouse fibroblast L2071 cells. This finding suggests that LPS has a potential role in tissue remodeling, wound healing, and various functional aspects related to fibroblast migration.

Here, we found that LPS induces intracellular calcium elevation in a unique way, i.e., LPS-induced  $\text{Ca}^{2+}$  response was desensitized by pretreating with LPS, S1P, or lysophosphatidic acid, but S1P- or lysophosphatidic acid-induced  $\text{Ca}^{2+}$  response was not desensitized by LPS pretreatment (Fig 3). These findings suggest that LPS has lysophosphatidic acid or S1P receptors or that LPS receptor(s) can be heterologous desensitized by lysophosphatidic acid or S1P in mouse fibroblasts. Several reports have suggested that LPS might have a unique cell surface receptor, i.e., one that differs from those of other lysolipids, such as S1P or lysophosphatidic acid (An et al., 1998; Bandoh et al., 1999; Okamoto et al., 1999; Gonda et al., 1999). An *et al*, found that LPS failed to stimulate serum responsive element-driven luciferase expression in  $\text{LPA}_1$  or  $\text{LPA}_2$ -transfected Jurkat cells (An et al., 1998), and Bandoh *et al*, reported that LPS failed to stimulate intracellular calcium increases in  $\text{LPA}_3$ -transfected Sf9 cells (Bandoh et al., 1999). These findings suggest that LPS is not a ligand for the three known lysophosphatidic acid receptors;  $\text{LPA}_1$ ,  $\text{LPA}_2$  and  $\text{LPA}_3$  (An et al., 1998; Bandoh et al., 1999). It has also been reported that LPS failed to inhibit the binding of [ $^{32}\text{P}$ ] S1P to S1P receptors or S1P-induced intracellular calcium

## MOL 18960

increases in S1P receptors-transfected cells (Okamoto et al., 1999; Gonda et al., 1999). In this study, we found that LPS-induced calcium signaling is not affected by VPC 32183, a lysophosphatidic acid receptor-selective antagonist (Fig 4). However, lysophosphatidic acid-induced intracellular calcium increases were completely inhibited by VPC 32183 (Fig. 4). These results strongly indicate that LPS has a unique cell surface receptor, and that it differs from lysophosphatidic acid receptors.

Furthermore, previously Xu et al. reported that pretreatment with lysophosphatidylglycerol (LPG), which has been shown to prevent the binding of lysophosphatidic acid to a putative cell-surface receptor, inhibited the calcium release induced by lysophosphatidic acid, but not that induced by LPS, in Jurkat T cells and HEY ovarian cancer cells (Xu et al., 1995a; Xu et al., 1995b), which also strongly suggests that LPS binds to a unique receptor different from lysophosphatidic acid receptors in Jurkat T cells and ovarian cancer cells. Taken together, it is evident that LPS has a unique cell surface receptor, which can be heterologously desensitized by lysophosphatidic acid or S1P receptor activation. We also investigated the effect of pertussis toxin, which specifically blocks the coupling of GPCRs to Gi, on LPS-induced signaling. When L2071 cells were treated with 100 ng/ml of pertussis toxin for 24 h prior to LPS stimulation, LPS-induced intracellular calcium elevation was not inhibited (Fig. 2B and 2C). However, the activations of ERK or p38 kinase and LPS-induced chemotactic migration were completely inhibited by pertussis toxin treatment, as shown in Figs. 6A and 9A. These results also imply that LPS utilizes pertussis toxin-sensitive G-protein-coupled receptor. In addition, we found that the overexpression of RGS4, a negative regulator of Gi and Gq, dramatically inhibited LPS-induced ERK phosphorylation, thus suggesting the crucial involvement of trimeric G-proteins in the ERK phosphorylation (Fig. 6B). Taken together, it appears that LPS stimulates at least two different G-protein-coupled signalings, i.e., pertussis toxin-insensitive G-protein-



## MOL 18960

mediated phospholipase C activation and intracellular calcium increase, and pertussis toxin-sensitive G-protein-mediated chemotactic migration via ERK and PI3K. To our knowledge this is the first report to demonstrate the role of trimeric G-proteins or G-protein coupled receptors in the LPS-induced stimulation of fibroblasts.

Our investigation of signals triggering LPS-induced chemotaxis in L2071 cells using specific inhibitors, such as, pertussis toxin, PD98059, LY294002 and Western blot analysis, identified the critical roles of pertussis toxin-sensitive G-proteins, ERK, and PI3K. The concentration-dependency of LPS-induced L2071 chemotaxis correlates well with the LPS-induced ERK and Akt phosphorylations. However, though phospholipase C-mediated calcium signaling pathway was not found to be involved in LPS-induced chemotaxis (data not shown), it might modulate the EC<sub>50</sub> values for chemotaxis and calcium release by LPS. In view of the fact that calcium signaling regulates various kinds of cellular physiologies and that LPS dramatically stimulates phospholipase C-mediated intracellular calcium increase, it would be interesting to determine the other functional roles of LPS in L2071 cells in relation to calcium signaling-dependent processes. This type of future work would probably reveal other important lipid-mediating roles of LPS.

In conclusion, the present study shows that LPS induces the chemotactic migration of L2071 mouse fibroblasts by modulating the activities of several intracellular signaling molecules like ERK and Akt, and of transmembrane signaling molecules, such as, pertussis toxin-sensitive trimeric G proteins and phospholipase C. Since this study is the first to describe the role of LPS in mouse fibroblast chemotaxis, further studies on the pathologic and physiologic roles of LPS and on its specific cell surface receptor(s) are required.

## References

- An S, Bleu T, Hallmark OG, and Goetzl EJ. (1998) Characterization of a novel subtype of human G protein-coupled receptor for lysophosphatidic acid. *J Biol Chem* **273**:7906-7910.
- An S, Bleu T, Zheng Y, and Goetzl EJ. (1998) Recombinant human G protein-coupled lysophosphatidic acid receptors mediate intracellular calcium mobilization. *Mol Pharmacol* **54**:881-888.
- Bae YS, Bae H, Kim Y, Lee TG, Suh PG, and Ryu SH. (2001) Identification of novel chemoattractant peptides for human leukocytes. *Blood* **97**:2854-2862.
- Bae YS, Kim Y, Kim Y, Kim JH, Suh PG, and Ryu SH. Trp-Lys-Tyr-Met-Val-D-Met is a chemoattractant for human phagocytic cells. *J Leukoc Biol* **66**:915-922.
- Bae YS, Yi HJ, Lee HY, Jo EJ, Kim JI, Lee TG, Ye RD, Kwak JY, and Ryu SH. (2003) Differential activation of formyl peptide receptor-like 1 by peptide ligands. *J Immunol* **171**:6807-6813.
- Bandoh K, Aoki J, Hosono H, Kobayashi S, Kobayashi T, Murakami-Murofushi K, Tsujimoto M, Arai H, and Inoue K. (1999) Molecular cloning and characterization of a novel human G-protein-coupled receptor, EDG7, for lysophosphatidic acid. *J Biol Chem* **274**:27776-27785.
- Berman DM, Wilkie TM, and Gilman AG. (1996) GAIP and RGS4 are GTPase-activating proteins for the Gi subfamily of G protein alpha subunits. *Cell* **86**:445-452.
- Fukushima N, Kimura Y, and Chun J. (1998) A single receptor encoded by vzg-1/lpA1/edg-2 couples to G proteins and mediates multiple cellular responses to lysophosphatidic acid. *Proc Natl Acad Sci U S A* **95**:6151-6156.
- Gonda K, Okamoto H, Takuwa N, Yatomi Y, Okazaki H, Sakurai T, Kimura S, Sillard R, Harii K, and Takuwa Y. (1999) The novel sphingosine 1-phosphate receptor AGR16 is

MOL 18960

- coupled via pertussis toxin-sensitive and -insensitive G-proteins to multiple signalling pathways. *Biochem J* **337**:67-75.
- Grynkiewicz G, Poenie M, and Tsien RY. (1985) A new generation of Ca<sup>2+</sup> indicators with greatly improved fluorescence properties. *J Biol Chem* **260**:3440-3450.
- Hama K, Aoki J, Fukaya M, Kishi Y, Sakai T, Suzuki R, Ohta H, Yamori T, Watanabe M, Chun J, and Arai H. (2004) Lysophosphatidic acid and autotaxin stimulate cell motility of neoplastic and non-neoplastic cells through LPA1. *J Biol Chem* **279**:17634-17639.
- Haribabu B, Zhelev DV, Pridgen BC, Richardson RM, Ali H, and Snyderman R. (1999) Chemoattractant receptors activate distinct pathways for chemotaxis and secretion. Role of G-protein usage. *J Biol Chem* **274**:37087-37092.
- Hla T and Maciag T. (1990) An abundant transcript induced in differentiating human endothelial cells encodes a polypeptide with structural similarities to G-protein-coupled receptors. *J Biol Chem* **265**:9308-9313.
- Hotary KB, Yana I, Sabeh F, Li XY, Holmbeck K, Birkedal-Hansen H, Allen ED, Hiraoka N, and Weiss SJ. (2002) Matrix metalloproteinases (MMPs) regulate fibrin-invasive activity via MT1-MMP-dependent and -independent processes. *J Exp Med* **195**:295-308.
- Huang C, Hepler JR, Gilman AG, and Mumby SM. (1997) Attenuation of Gi- and Gq-mediated signaling by expression of RGS4 or GAIP in mammalian cells. *Proc Natl Acad Sci U S A* **94**:6159-6163.
- Ignatov A, Lintzel J, Hermans-Borgmeyer I, Kreienkamp HJ, Joost P, Thomsen S, Methner A, and Schaller HC. (2003) Role of the G-protein-coupled receptor GPR12 as high-affinity receptor for sphingosylphosphorylcholine and its expression and function in brain development. *J Neurosci* **23**:907-914.
- Im DS, Fujioka T, Katada T, Kondo Y, Ui M, and Okajima F. (1997) Characterization of sphingosine 1-phosphate-induced actions and its signaling pathways in rat hepatocytes.

MOL 18960

*Am J Physiol* **272**:G1091-G1099.

Johnson GL and Lapadat R. Mitogen-activated protein kinase pathways mediated by ERK, JNK, and p38 protein kinases. *Science* **298**:1911-1912.

Kawamoto K, Aoki J, Tanaka A, Itakura A, Hosono H, Arai H, Kiso Y, and Matsuda H. (2002) Nerve growth factor activates mast cells through the collaborative interaction with lysophosphatidylserine expressed on the membrane surface of activated platelets. *J Immunol* **168**:6412-6419.

Kim JI, Jo EJ, Lee HY, Cha MS, Min JK, Choi CH, Lee YM, Choi YA, Baek SH, Ryu SH, Lee KS, Kwak JY, and Bae YS. (2003) Sphingosine 1-phosphate in amniotic fluid modulates cyclooxygenase-2 expression in human amnion-derived WISH cells. *J Biol Chem* **278**:31731-31736.

Kon J, Sato K, Watanabe T, Tomura H, Kuwabara A, Kimura T, Tamama K, Ishizuka T, Murata N, Kanda T, Kobayashi I, Ohta H, Ui M, and Okajima F. (1999) Comparison of intrinsic activities of the putative sphingosine 1-phosphate receptor subtypes to regulate several signaling pathways in their cDNA-transfected Chinese hamster ovary cells. *J Biol Chem* **274**:23940-23947.

Kundra V, Escobedo JA, Kazlauskas A, Kim HK, Rhee SG, Williams LT, and Zetter BR. (1994) Regulation of chemotaxis by the platelet-derived growth factor receptor-beta. *Nature* **367**:474-476.

Lachance G, Levasseur S, and Naccache PH. (2002) Chemotactic factor-induced recruitment and activation of Tec family kinases in human neutrophils. Implication of phosphatidylinositol 3-kinases. *J Biol Chem* **277**:21537-21541.

Liliom K, Guan Z, Tseng JL, Desiderio DM, Tigyi G, and Watsky MA. (1998) Growth factor-like phospholipids generated after corneal injury. *Am J Physiol* **274**:C1065-C1074.

Lee MJ, Thangada S, Claffey KP, Ancellin N, Liu CH, Kluk M, Volpi M, Sha'afi RI, and Hla

MOL 18960

- T. (1999) Vascular endothelial cell adherens junction assembly and morphogenesis induced by sphingosine-1-phosphate. *Cell* **99**:301-312.
- Lee MJ, Van Brocklyn JR, Thangada S, Liu CH, Hand AR, Menzeleev R, Spiegel S, and Hla T. (1998) Sphingosine-1-phosphate as a ligand for the G protein-coupled receptor EDG-1. *Science* **279**:1552-1555.
- Lourenssen S, and Blennerhassett MG (1998) Lysophosphatidylserine potentiates nerve growth factor-induced differentiation of PC12 cells. *Neurosci Lett* **248**:77-80.
- Morales-Ruiz M, Lee MJ, Zollner S, Gratton JP, Scotland R, Shiojima I, Walsh K, Hla T, and Sessa WC. (2001) Sphingosine 1-phosphate activates Akt, nitric oxide production, and chemotaxis through a Gi protein/phosphoinositide 3-kinase pathway in endothelial cells. *J Biol Chem* **276**:19672-19677.
- Murrin RJ and Boarder MR. (1992) Neuronal "nucleotide" receptor linked to phospholipase C and phospholipase D? Stimulation of PC12 cells by ATP analogues and UTP. *Mol Pharmacol* **41**:561-568.
- Noguchi K, Ishii S, and Shimizu T. (2003) Identification of p2y9/GPR23 as a novel G protein-coupled receptor for lysophosphatidic acid, structurally distant from the Edg family. *J Biol Chem* **278**:25600-25606.
- Noh DY, Shin SH, and Rhee SG. (1995) Phosphoinositide-specific phospholipase C and mitogenic signaling. *Biochim Biophys Acta* **1242**:99-113.
- Okamoto H, Takuwa N, Yatomi Y, Gonda K, Shigematsu H, and Takuwa Y. (1999) EDG3 is a functional receptor specific for sphingosine 1-phosphate and sphingosylphosphorylcholine with signaling characteristics distinct from EDG1 and AGR16. *Biochem Biophys Res Commun* **260**:203-208.
- Sato T, Aoki J, Nagai Y, Dohmae N, Takio K, Doi T, Arai H, and Inoue K. (1997) Serine phospholipid-specific phospholipase A that is secreted from activated platelets. A new

MOL 18960

- member of the lipase family. *J Biol Chem* **272**:2192-2198.
- Soga T, Ohishi T, Matsui T, Saito T, Matsumoto M, Takasaki J, Matsumoto S, Kamohara M, Hiyama H, Yoshida S, Momose K, Ueda Y, Matsushime H, Kobori M, and Furuichi K. (2005) Lysophosphatidylcholine enhances glucose-dependent insulin secretion via an orphan G-protein-coupled receptor. *Biochem Biophys Res Commun* **326**:744-751.
- Tigyi G, Dyer DL, and Miledi R. (1994) Lysophosphatidic acid possesses dual action in cell proliferation. *Proc Natl Acad Sci U S A* **91**:1908-1912.
- van Corven EJ, Groenink A, Jalink K, Eichholtz T, and Moolenaar WH. (1989) Lysophosphatide-induced cell proliferation: identification and dissection of signaling pathways mediated by G proteins. *Cell* **59**:45-54.
- Wang C, Hayashi H, Harrison R, Chiu B, Chan JR, Ostergaard HL, Inman RD, Jongstra J, Cybulsky MI, and Jongstra-Bilen J. (2002) Modulation of Mac-1 (CD11b/CD18)-mediated adhesion by the leukocyte-specific protein 1 is key to its role in neutrophil polarization and chemotaxis. *J Immunol* **169**:415-423.
- Wang L, Knudsen E, Jin Y, Gessani S, and Maghazachi AA. (2004) Lysophospholipids and chemokines activate distinct signal transduction pathways in T helper 1 and T helper 2 cells. *Cell Signal* **16**:991-1000.
- Wilberding JA, Ploplis VA, McLennan L, Liang Z, Cornelissen I, Feldman M, Deford ME, Rosen ED, and Castellino FJ. (2001) Development of pulmonary fibrosis in fibrinogen-deficient mice. *Ann N Y Acad Sci* **936**:542-548.
- Xu Y, Casey G, and Mills GB. (1995b) Effect of lysophospholipids on signaling in the human Jurkat T cell line. *J Cell Physiol* **163**:441-450.
- Xu Y, Fang XJ, Casey G, and Mills GB. (1995a) Lysophospholipids activate ovarian and breast cancer cells. *Biochem J* **309**:933-940.
- Xu Y, Zhu K, Hong G, Wu W, Baudhuin LM, Xiao Y, and Damron DS. (2000)

MOL 18960

Sphingosylphosphorylcholine is a ligand for ovarian cancer G-protein-coupled receptor 1.

*Nat Cell Biol* **2**:261-267.

Zhu K, Baudhuin LM, Hong G, Williams FS, Cristina KL, Kabarowski JH, Witte ON, and Xu

Y. (2001) Sphingosylphosphorylcholine and lysophosphatidylcholine are ligands for the G protein-coupled receptor GPR4. *J Biol Chem* **276**:41325-41335.

## Footnotes

This work was supported by the Korea Science and Engineering Foundation through the Medical Science and Engineering Research Center for Cancer Molecular Therapy at Dong-A University, the Korea Science and Engineering Foundation Grant (R01-2005-000-10011-02005), and a grant A050027 from the Korea Health 21 R&D Project, Ministry of Health & Welfare, Republic of Korea.

Address reprints request to Dr. Yoe-Sik Bae, Medical Research Center for Cancer Molecular Therapy and Department of Biochemistry, College of Medicine, Dong-A University, Busan 602-714, Korea. E-mail address: yoesik@donga.ac.kr



## Figure legends

**Fig. 1.** The effect of LPS on intracellular calcium elevation in L2071 cells. L2071 cells were stimulated with 2  $\mu$ M of LPS or 2  $\mu$ M of LPE and intracellular calcium levels were determined fluorometrically using fura-2/AM. Relative intracellular calcium concentrations are expressed as fluorescence ratios (340:380 nm). Data are representative of five independent experiments (A). L2071 cells were stimulated with various concentrations of LPS or LPE, and peak intracellular calcium levels were recorded. Results are presented as means  $\pm$  SE of three independent experiments performed in duplicate (B). \* Statistically significant ( $P < 0.05$ ) from the control (0.1 nM treated).

**Fig. 2.** LPS-induced  $\text{Ca}^{2+}$  signaling is U-73122-sensitive but pertussis toxin-insensitive in L2071 cells. L2071 cells were pretreated with 5  $\mu$ M of U73122 or 5  $\mu$ M of U73343 prior to 2  $\mu$ M of LPS, and intracellular calcium levels were determined (A). L2071 cells were preincubated in the absence or presence of 100 ng/ml of pertussis toxin for 24 h, loaded with fura-2/AM, and intracellular calcium levels were determined fluorometrically after adding 2  $\mu$ M of LPS or 1  $\mu$ M of leukotriene B4 (B). L2071 cells were preincubated in the absence or presence of 100 ng/ml of pertussis toxin for 24 h, and intracellular calcium levels were determined fluorometrically after adding various concentrations of LPS (C) Relative intracellular calcium concentrations are expressed as fluorescence ratios (340:380 nm). Data are representative of four independent experiments (A, B, C).

**Fig. 3.** LPS induces intracellular calcium elevation via unique receptor(s) in L2071 cells. Intracellular calcium concentrations were determined fluorometrically using fura-2/AM, as described in "Materials and methods." Cells were challenged with 2  $\mu$ M LPS or 5  $\mu$ M LPA

# MOL 18960

(A), and fura-2/AM loaded L2071 cells were challenged with 2  $\mu$ M LPS or 2  $\mu$ M S1P at the times indicated (B). L2071 cells were pretreated with 2  $\mu$ M LPS for 3 min and then stimulated with various concentrations of LPA (C) or S1P (D). Relative intracellular calcium concentrations are expressed as fluorescence ratios (340:380 nm). The tracings shown are from one experiment representative of at least four separate experiments (A, B). Results are presented as means  $\pm$  SE of three independent experiments performed in duplicate (C, D).

**Fig. 4.** LPS-induced intracellular calcium increases are not inhibited by lysophosphatidic acid receptor antagonist. Intracellular calcium concentrations were determined fluorometrically using fura-2/AM, as described in “Materials and methods.” Cells were challenged with vehicle (DW), 1  $\mu$ M LPA, or 1  $\mu$ M VPC 32183 (A), and fura-2/AM loaded L2071 cells were challenged with vehicle (DW), 1  $\mu$ M LPS, or 1  $\mu$ M VPC 32183 at the times indicated (B). Cells were stimulated with vehicle (DW) or 1  $\mu$ M VPC 32183 before adding LPS (C). Relative intracellular calcium concentrations are expressed as fluorescence ratios (340:380 nm). The tracings shown are representative of at least four separate experiments (A, B). Results are presented as the means  $\pm$  SE of three independent experiments performed in duplicate (C).

**Fig. 5.** LPS stimulates MAPK phosphorylation in L2071 cells. L2071 cells were stimulated with 2  $\mu$ M LPS for various times (A), and then stimulated with various concentrations of LPS for 2min (B). Samples (30  $\mu$ g of protein) were subjected to 10% SDS-PAGE, and phosphorylated ERK or p38 kinase levels were determined by immunoblotting using anti-phospho-ERK antibody or anti-phospho-p38 kinase antibody. The results shown are representative of at least three independent experiments.

**Fig. 6.** LPS-induced MAPKs phosphorylation is mediated by pertussis toxin-sensitive G-protein. L2071 cells, preincubated in the absence or presence of 100 ng/ml of pertussis toxin for 24 h, were stimulated with 2  $\mu$ M LPS for 5 min (A). Vector- or HA-tagged human RGS-4-transfected L2071 cells were treated with 2  $\mu$ M LPS for various times (B). Immunoblot analysis with anti-phospho-ERK antibodies was performed on lysates, and immunoblot analysis with anti-ERK antibody was used to confirm equal protein loadings. The results shown are representative of at least three independent experiments.

**Fig. 7.** LPS stimulates Akt phosphorylation in a pertussis toxin-sensitive manner in L2071 cells. L2071 cells were stimulated with 2  $\mu$ M LPS for various times (A), and then stimulated with various concentrations of LPS for 5min (B). L2071 cells, preincubated in the presence of 100 ng/ml of pertussis toxin for 24h, were stimulated with either 2  $\mu$ M of LPS for various times (C) or with various concentrations of LPS for 5min (D). Samples (30  $\mu$ g of protein) were subjected to 10% SDS-PAGE, and phosphorylated Akt levels were determined by immunoblotting using anti-phospho-Akt antibody. The results shown are representative of at least three independent experiments.

**Fig. 8.** LPS induces L2071 cell chemotaxis. Assays were performed using a modified Boyden chamber assay as described in “Materials and methods”. The polycarbonate membrane of a 96-well chemotaxis chamber was precoated with BSA (2%), fibrinogen (20  $\mu$ g/ml), or fibronectin (20  $\mu$ g/ml) in carbonate buffer (500 mM sodium bicarbonate, pH 8.5) overnight at room temperature. Cultured L2071 cells ( $1 \times 10^6$  cells/ml in serum free RPMI) were added to the upper well of the 96-well chemotaxis chamber and migration across a polycarbonate

MOL 18960

membrane of 8  $\mu\text{m}$  pore size was assessed in the presence of 2  $\mu\text{M}$  LPS for 4 h at 37°C (A). Various concentrations of LPS were used to examine chemotactic migration using fibronectin (20  $\mu\text{g/ml}$ ) precoated polycarbonate membranes (B). Migrated cell numbers were counted in 3 high power fields (400x). Data are presented as the means  $\pm$  SE of three independent experiments performed in duplicate. \* Significantly different ( $P < 0.05$ ) from the control (vehicle treated).

**Fig. 9.** LPS-induced L2071 chemotaxis is mediated by pertussis toxin-sensitive G-proteins, PI3K, and ERK. The polycarbonate membrane of a 96-well chemotaxis chamber was precoated with fibronectin (20  $\mu\text{g/ml}$ ) in carbonate buffer (500 mM sodium bicarbonate, pH 8.5) overnight at room temperature. L2071 cells, preincubated in the absence or presence of 100 ng/ml of pertussis toxin for 24 h, were subjected to chemotaxis assays at LPS concentrations of 0, 2, and 5  $\mu\text{M}$  (A). \* Significantly different ( $P < 0.05$ ) from the control (-pertussis toxin). L2071 cells were treated with vehicle (DMSO), PD098059 (50  $\mu\text{M}$ ), SB203580 (20  $\mu\text{M}$ ), or LY294002 (50  $\mu\text{M}$ ) for 15 min, and then subjected to chemotaxis assays in the presence of 2  $\mu\text{M}$  LPS for 4 h (B). Migrated cell numbers were counted in 3 high power fields (400x). Data are presented as the means  $\pm$  SE of three independent experiments performed in duplicate (A, B). \* Significantly different ( $P < 0.05$ ) from the control (DMSO treated).

MOL 18960

Table 1. The Migration of L2071 cell across a Polycarbonate Membrane after LPS treatment<sup>a</sup>

Above Membrane (μM)	Below Membrane (μM)				
	0	0.1	1	2	5
0	28 ± 4	26 ± 7	32 ± 5	29 ± 3	31 ± 8
5	131 ± 18	125 ± 26	87 ± 11	54 ± 8	34 ± 3

<sup>a</sup> L2071 cell migration was analyzed for 4 h across a fibronectin-coated polycarbonate membrane (8 μm pore size). Different LPS concentrations were placed in the lower compartment in the absence or presence of LPS (5 μM) in the above compartments. Data are represent the means ± SE of migrated L2071 cell numbers in 3 high power fields (400x) counted in triplicate for two independent experiments.

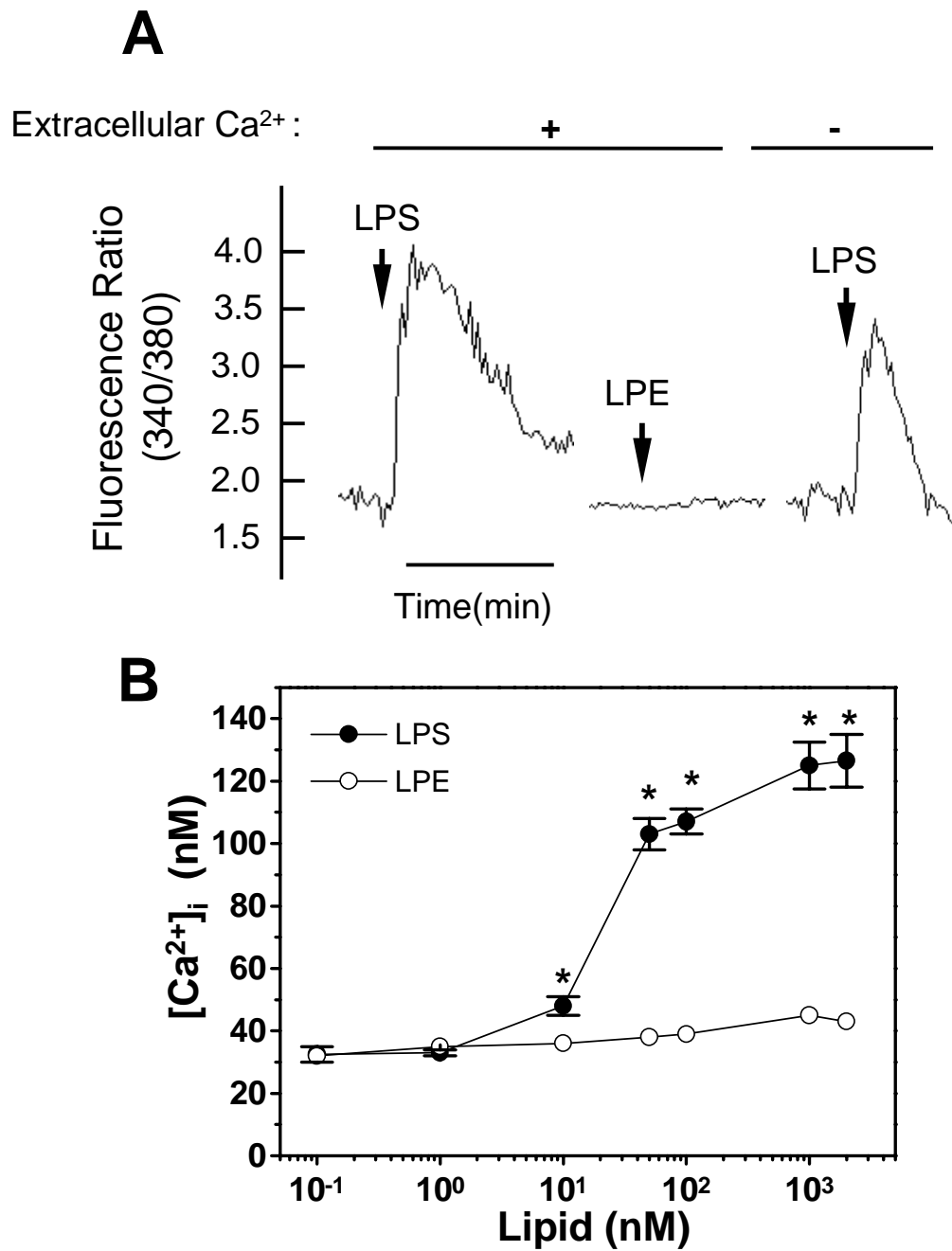
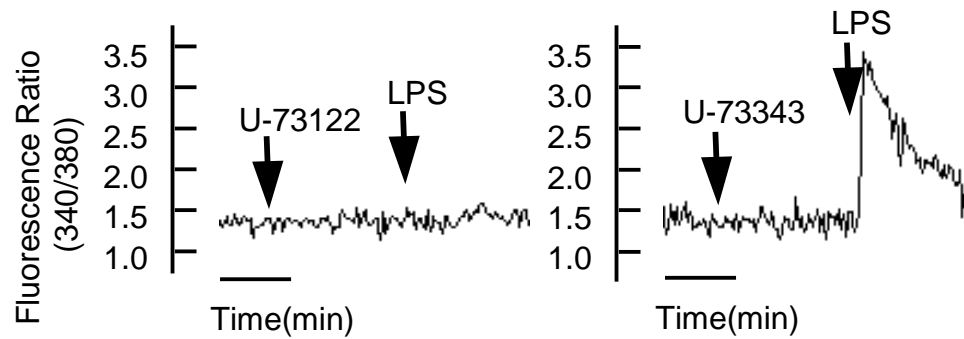
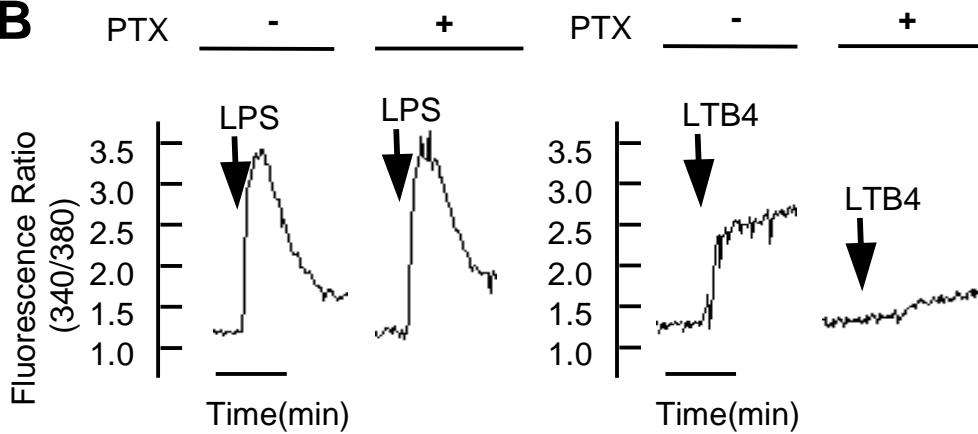


Fig. 1

**A**



**B**



**C**

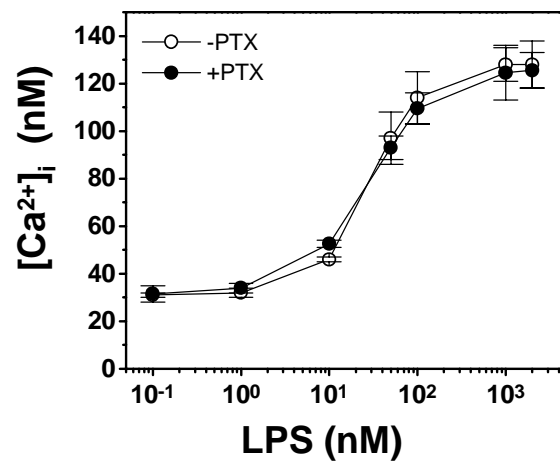


Fig. 2

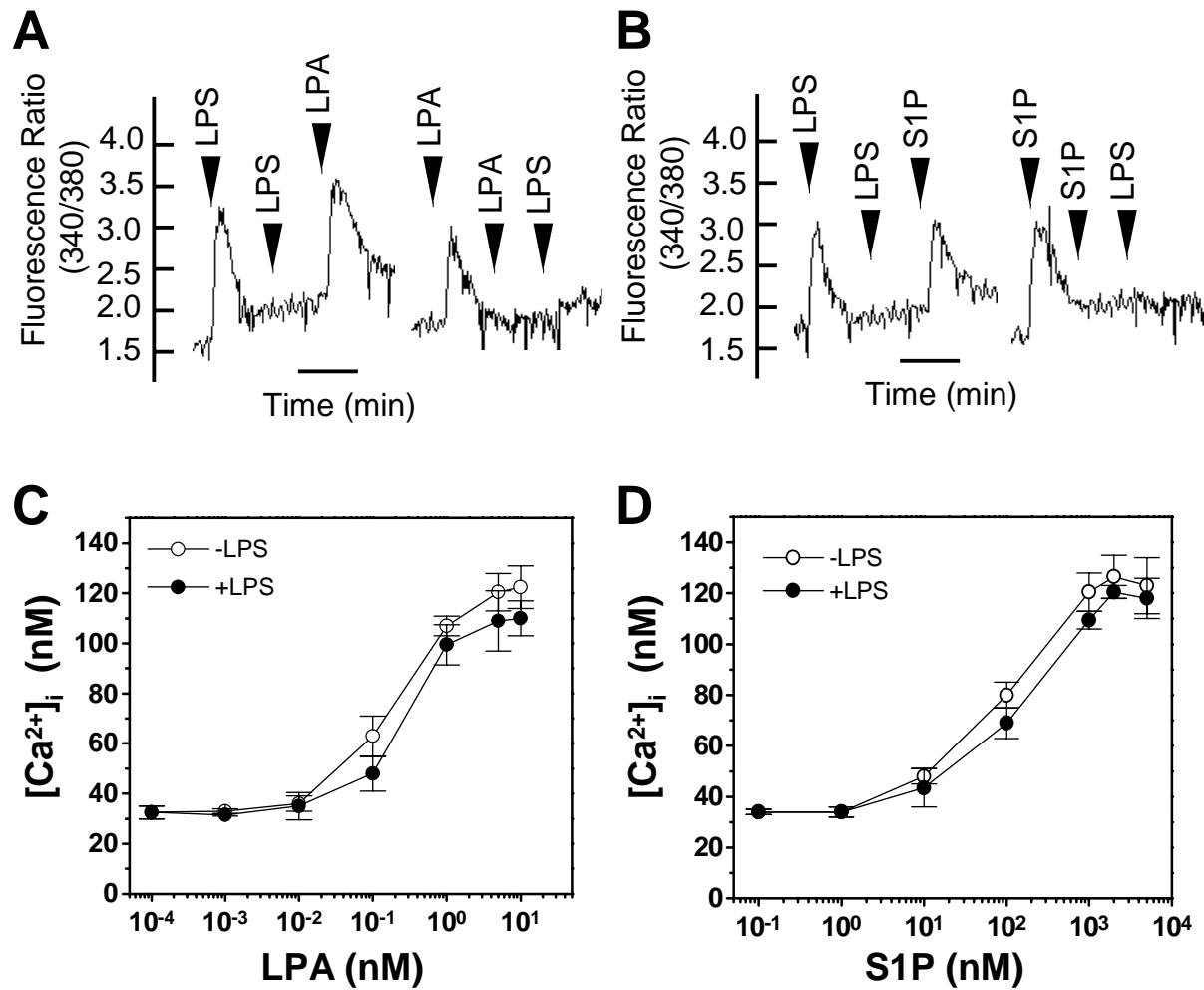


Fig. 3



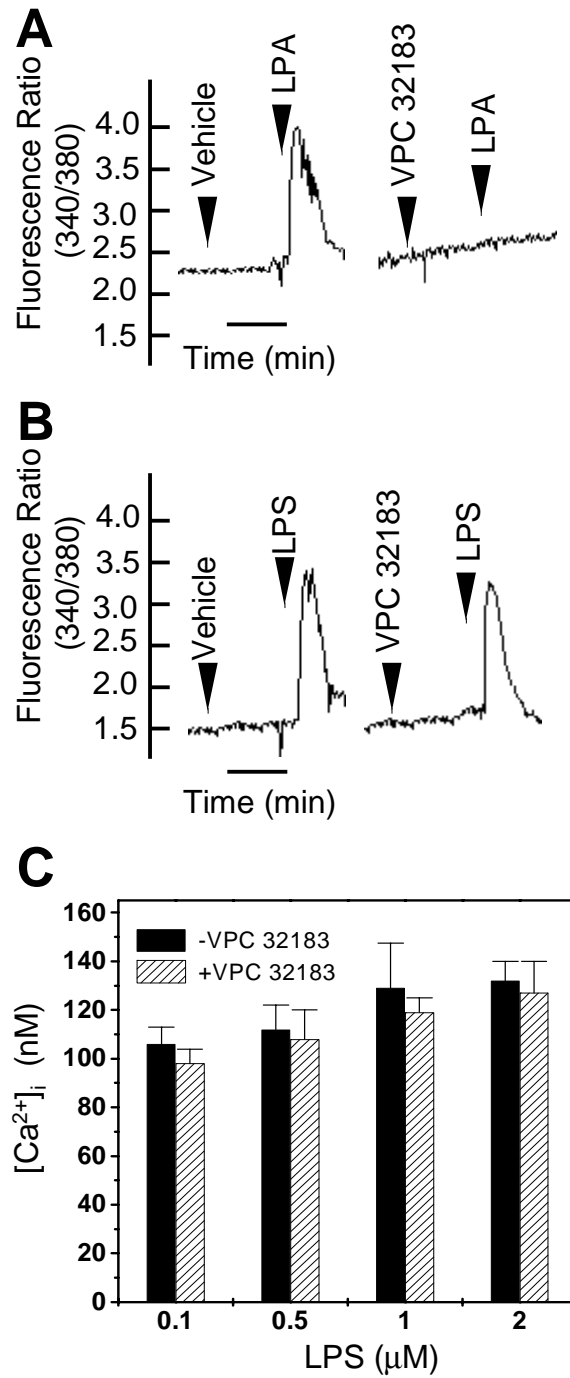


Fig. 4

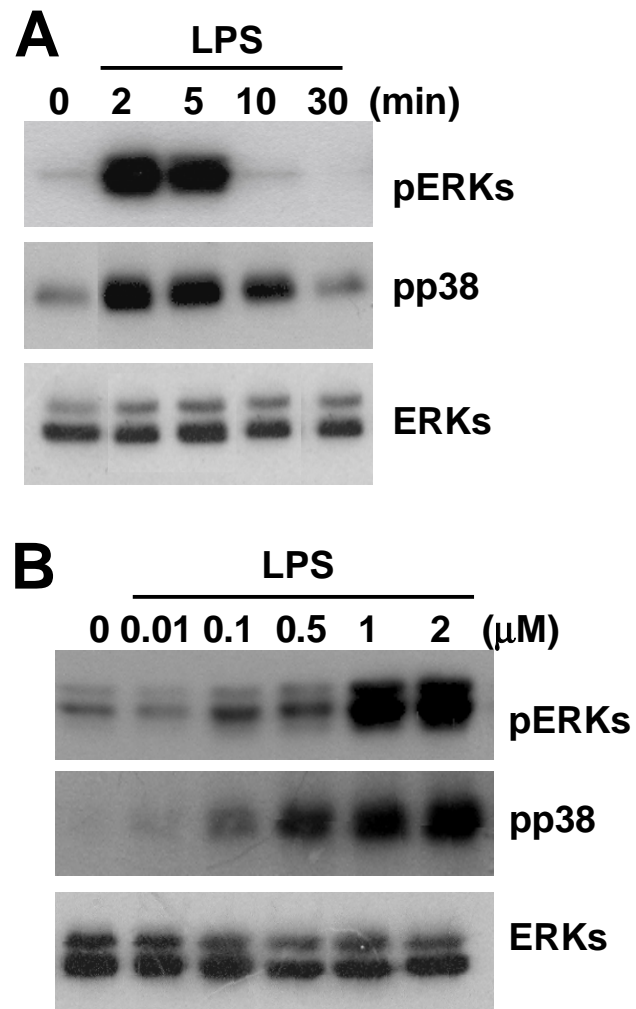


Fig. 5

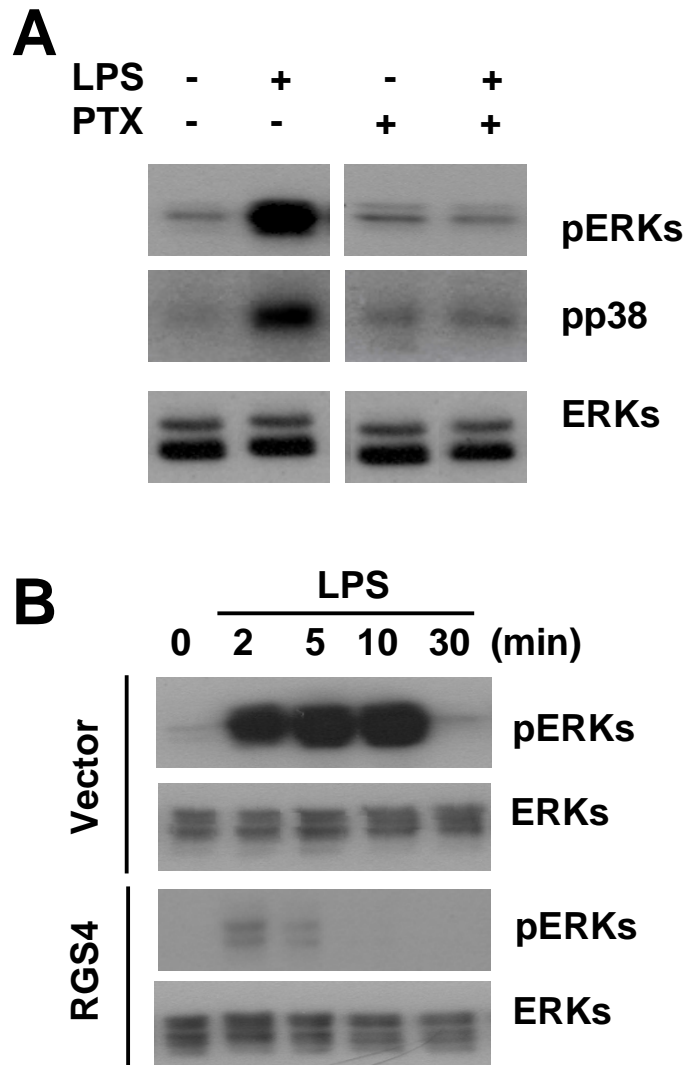


Fig. 6

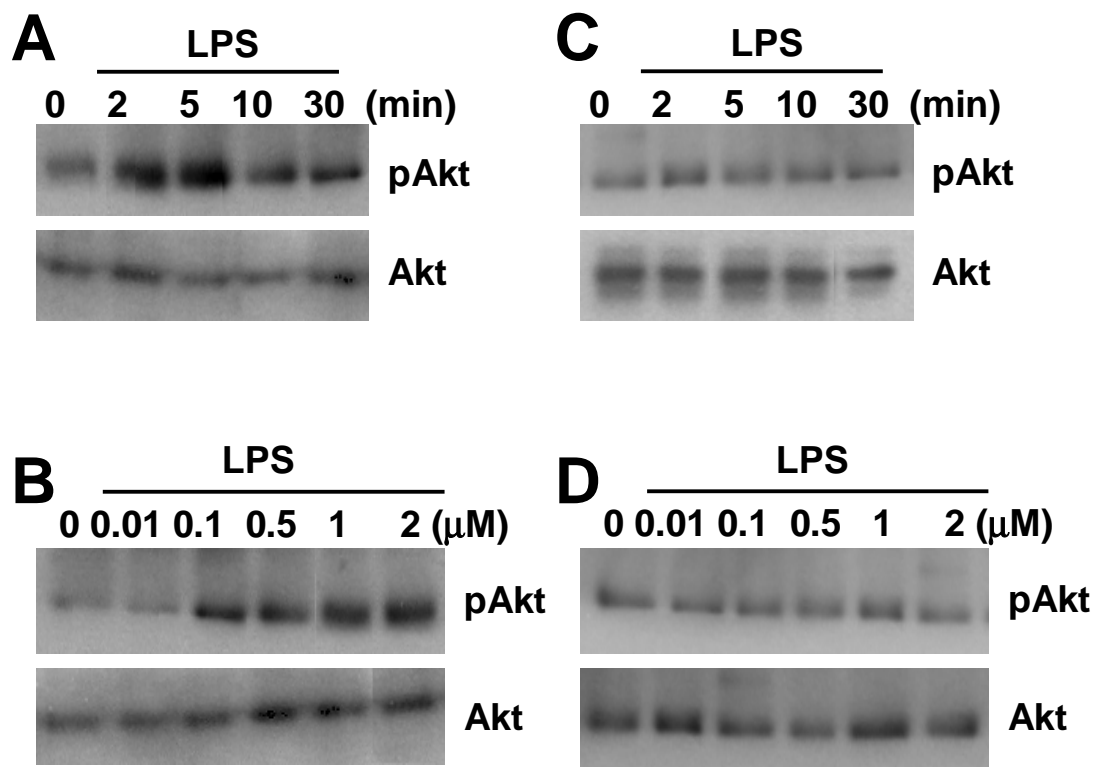


Fig. 7

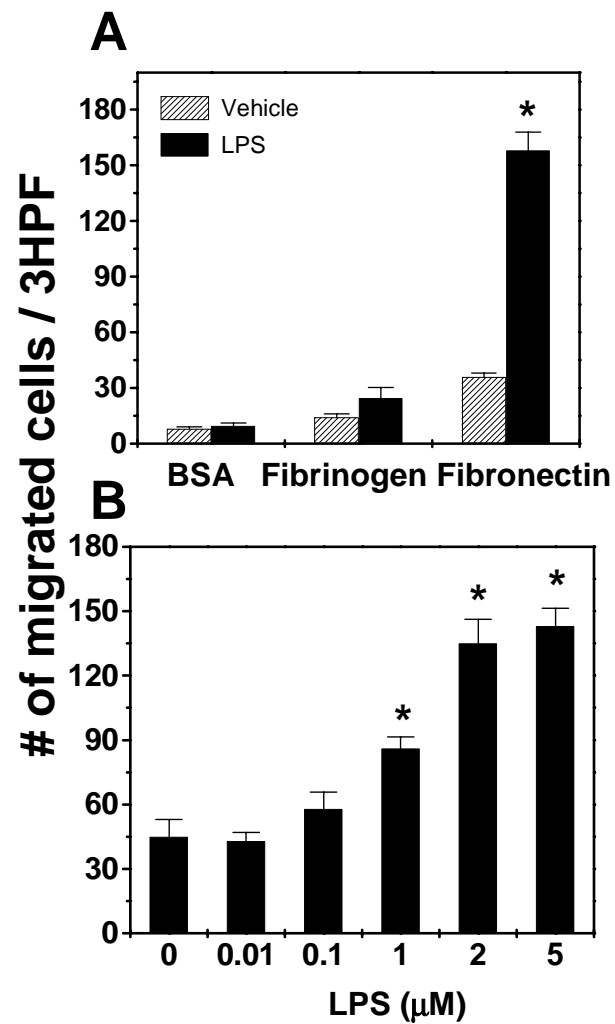


Fig. 8

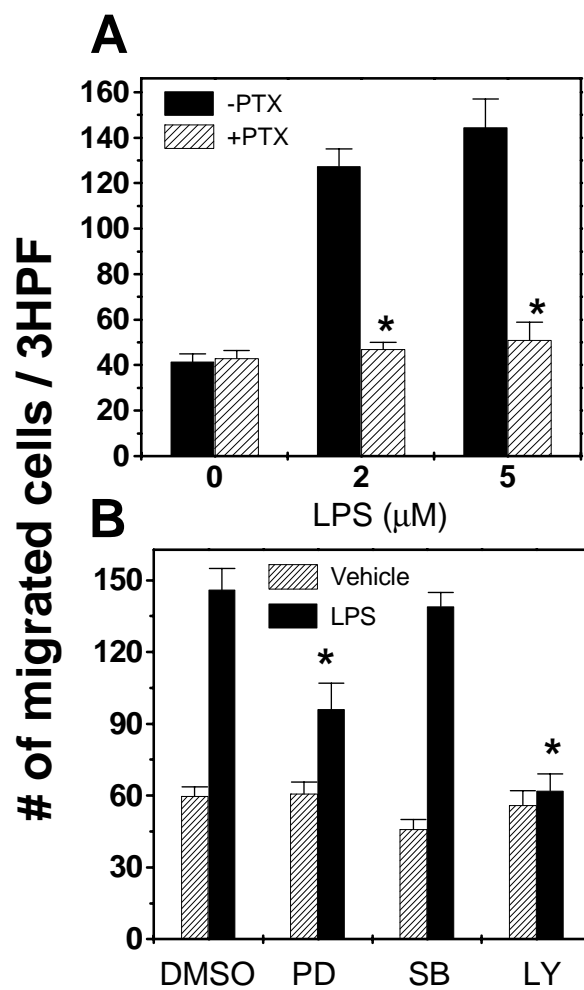


Fig. 9